FIRST-PRINCIPLES CALCULATIONS OF THE STRUCTURAL, ELECTRONIC AND ELASTIC PROPERTIES OF $SrGeO_3$ AND $SrZrO_3$ CUBIC PEROVSKITES

Mikhail G. BRIK[1], Nicolae M. AVRAM[2], Calin N. AVRAM[3]

Abstract. *The structural, electronic, elastic and thermodynamic properties of two cubic perovskites – $SrGeO_3$ and $SrZrO_3$ – were calculated using the first-principles methods for the pressure range from 0 to 25 GPa. Comparison of the calculated results with other literature data (whether available) yielded good agreement. Dependencies of all calculated properties – such as lattice constants, relative change of the unit cell volume, elastic constants and Debye temperature – on pressure were obtained, which enables reliable estimations of all these parameters for any value of hydrostatic pressure in the studied range.*

Keywords: Perovskite; First-principles calculations; Electronic properties; Elastic properties

1. Introduction

Perovskites is a common name for a large group of compounds with the general chemical formulas ABX_3 (if A and B are the di- and tetravalent metals, then X is oxygen; if A and B are the mono- and divalent metals, then X is a halogen). The possible combinations of these chemical elements should satisfy the stability criterion: the so called Goldschmidt tolerance factor $t = \frac{r_A + r_X}{\sqrt{2}\,(r_B + r_X)}$ (r_i is the ionic radius, the subscript i denotes an element in the chemical formula) should be confined in the range between 0.75 and 1 [1,2,3]. It is also possible to make the doubled perovskites $A_2BB'X_6$ by doubling a unit cell of an ABX_3 perovskite along the c crystallographic direction [4]. Versatile chemical composition of perovskites and their ability to accommodate organic complexes instead of some cations may also lead to a variety of stable crystallographic structures, such as cubic, rhombohedral, tetragonal, orthorhombic, and monoclinic.

[1]Prof., Dr. hab., College of Sciences & CQUPT-BUL Innovation Institute, Chongqing University of Posts and Telecommunications, Chongqing, 400065, People's Republic of China; Institute of Physics, University of Tartu, W. Ostwald Str. 1, Tartu, 50411, Estonia; Institute of Physics, Jan Dlugosz University, PL-42200, Czestochowa, Poland, (e-mail: mikhail.brik@ut.ee).
[2]Prof., PhD, Department of Physics, West University of Timisoara, Bd. V. Parvan, No. 4, 300223, Timisoara, Romania and Academy of Romanian Scientist, Independentei 54, 050094, Bucharest, Romania (e-mail: n1m2marva@yahoo.com).
[3] Assistant Prof., PhD, Department of Physics, West University of Timisoara, Bd. V. Parvan, No. 4, 300223, Timisoara, Romania (e-mail: calin.avram@e-uvt.ro).

Applications of the perovskite compounds are numerous. Some examples that prove technological importance of perovskites can be mentioned as follows: photovoltaics [5], magnetoresistive materials [6], fuel cells [7], lighting and display materials [8], catalysts [9], scintillators [10,11] etc.

Due to a very wide area of use and applications, various representatives of perovskite family were subjected to scrutinized theoretical studies, especially by means of the modern computational approaches based on the density functional theory (DFT). For example, surface terminations of $SrTiO_3$ were analyzed in Ref. [12], systematic studies of various ABO_3 perovskites surfaces described in Refs. [13,14, 15]; bulk electronic structures for $BaTiO_3$ and $SrTiO_3$ were calculated in Refs. [16] and [17,18], respectively; bulk properties of $ASnX_3$ (A=Rb, K; X=Cl, Br) were analyzed in Ref. [19] etc. Computational methods have also been proved to be efficient in predicting new materials with perovskite structures at extreme pressures [20,21].

Nowadays comparative studies of several or even more isostructural compounds acquire special importance, since they allow for uncovering certain "structure – property" and "property – property" trends, which can be useful guides in a search for new materials with improved performance. Such calculations are very popular now, which can be proved by a large number of publications on this topic [22,23, 24, 25, 26, 27, 28 etc.]. In the present paper we continue this line of research and perform the detailed calculations of the structural, electronic, elastic and thermodynamic properties of two cubic perovskites $SrGeO_3$ and $SrZrO_3$ to see how the change of the second cation affects the above mentioned properties.

In the next sections we describe the structure of the studied crystals, method of calculations and the obtained results before concluding a paper with a short summary.

2. Crystal structure of cubic $SrGeO_3$ and $SrZrO_3$ and details of calculations

Cubic perovskites $SrGeO_3$ and $SrZrO_3$ crystallize in the cubic space group Pm-3m, No. 221 [29,30]. The Ge (or Zr) atoms are six-fold coordinated by the oxygen ions, which form an ideal octahedron. The Sr ions are located in the cavities between the SrO_6 (ZrO_6) octahedra and are 12-fold coordinated by the oxygen ions, as shown in Fig. 1a.

All calculations were performed using the CASTEP module [31] of Materials Studio. Both generalized gradient approximation (GGA) [32] and local density approximation (LDA) [33,34] were used to treat electron correlation effects. The ultrasoft pseudopotentials were employed for a description of interaction between the ionic cores and valence electrons. The electron configurations were as follows: $4s^24p^65s^2$ for Sr; $4s^24p^64d^25s^2$ for Zr; $4s^24p^2$ for Ge and $2s^22p^4$ for O. The plane-

wave bases cut-off energy was 380 eV for both crystals. The k-points grid was 8×8×8; the convergence criteria were set as 5×10^{-6} eV/atom for energy, 0.01 eV/Å for maximal force, 0.02 GPa for maximal stress and 5×10^{-4} Å for maximal displacement. The calculated electronic structures were analyzed along the directions in the reciprocal space determined by the high-symmetry points of the Brillouin zone (Fig. 1b).

To analyze the pressure effects on the calculated properties, all calculations runs were performed at the ambient and elevated hydrostatic pressures up to 25 GPa, with a step of 5 GPa.

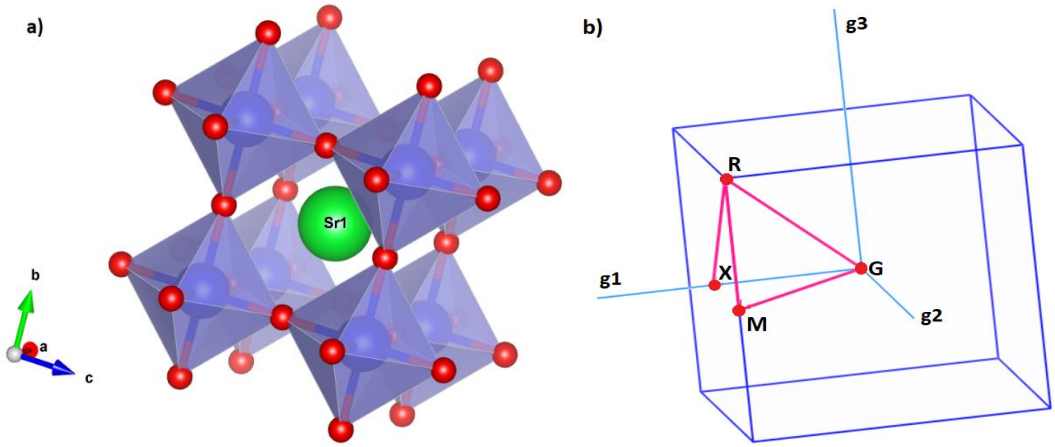

Fig. 1. a) One unit cell of $SrZrO_3$. Coordination octahedra around Zr ions are shown. Drawn with VESTA [35]. b) Brillouin zone for a unit cell of $SrZrO_3$ with indication of the high symmetry points, whose coordinates in units of the reciprocal lattice unit vectors are as follows: G(0, 0, 0); R(½, ½, ½); X(½, 0, 0); M(½, ½, 0).

3. Results of calculations

3.1. Structural properties

The optimized lattice constants for the considered in the present paper perovskites in comparison with the experimental data and other calculations are collected in Table 1.

As seen from Table 1, the $SrZrO_3$ lattice constant is greater than the $SrGeO_3$ because of a large ionic radius of the six-fold coordinated Zr ion (0.72 Å) in comparison with that for Ge (0.53 Å) [36]. Agreement between the experimental and calculated in this work lattice constants is good; the obtained results are also consistent with others reported in the literature.

Table 1) Calculated and experimental structural constants (in Å) for $SrGeO_3$ and $SrZrO_3$ cubic perovskites.

	Exp.	*Calc. (this work)*		*Calc. (other works)*			
		GGA	*LDA*				
$SrGeO_3$	3.7946 [a]	3.8563	3.7308	3.8029 [c]	3.859 [d]	3.78 [e]	3.896 [f]
$SrZrO_3$	4.0930 [b]	4.1712	4.0953	4.1794 [g]	4.1574 [h]	4.174 [i]	4.157 [j]

[a] Ref. [29] [b] Ref. [30] [c] Ref. [37] [d] Ref. [38] [e] Ref. [39] [f] Ref. [40] [g] Ref. [41] [h] Ref. [42] [i] Ref. [43] [j] Ref. [44]

Application of the external hydrostatic pressure will lead to a decrease of the lattice constants, which is illustrated by Fig. 2.

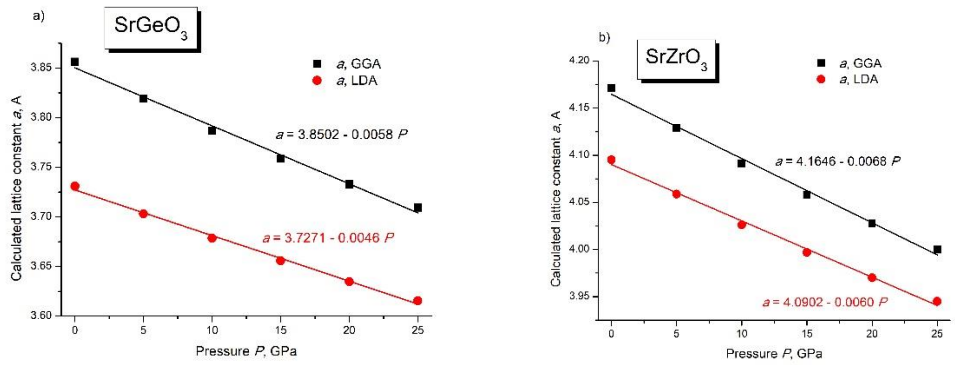

Fig. 2. Dependence of the calculated lattice constants on external hydrostatic pressure P for $SrGeO_3$ (a) and $SrZrO_3$ (b). The calculated values are shown by symbols, the linear fits are shown by straight lines. The fits equations are given in the graphs.

The lattice constants decrease is well approximated by the linear fits, with the slopes of about 0.005 – 0.007 Å/GPa. The $SrZrO_3$ appears to be somewhat more compressible than $SrGeO_3$, which is due to the increased interionic distances and softer chemical bonds in the former material.

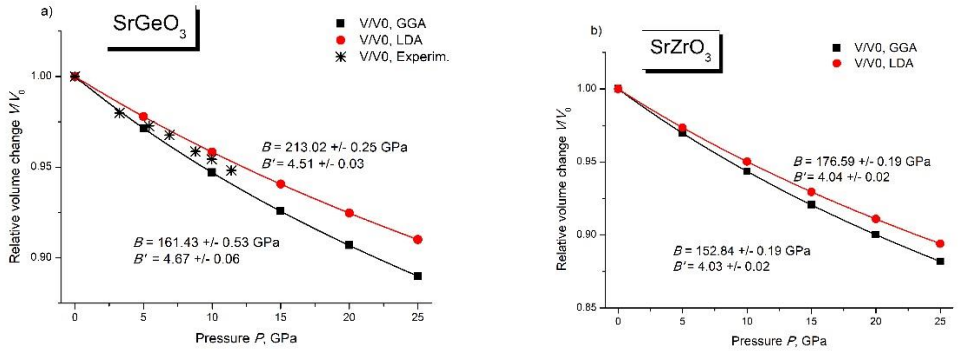

Fig. 3. Dependence of the calculated relative volume change of a unit cell on external hydrostatic pressure for $SrGeO_3$ (a) and $SrZrO_3$ (b). The calculated values are shown by symbols, the fits to the Murnaghan equation of state are shown by straight lines. The estimated bulk modulus B and its pressure derivative B' are given in the graphs.

Higher compressibility of $SrZrO_3$ is confirmed by the data presented in Fig. 3, which shows the relative change of the unit cell volume V/V_0 (where V and V_0 are the unit cell volume at pressure P and ambient pressure, respectively). The values of the V/V_0 ratio were fitted to the Murnaghan equation of state [45]

$$\frac{V}{V_0} = \left(1 + B'\frac{P}{B}\right)^{-\frac{1}{B'}}, \qquad (1)$$

where B is the bulk modulus and B' is its pressure derivative. The obtained values of these elastic constants are given in Figs 3a and 3b. In addition, the experimental data on change of the relative volume of a unit cell for $SrGeO_3$ at different pressures [40] are shown in Fig. 3a by the stars. Very good agreement between the calculated and experimental data was demonstrated. Unfortunately, no experimental data on compressibility of $SrZrO_3$ were found in the literature.

3.2. Electronic properties

The calculated band structures of both perovskites are shown in Fig. 4. It is known that the DFT-calculated band gaps are underestimated if compared with the experimental ones.

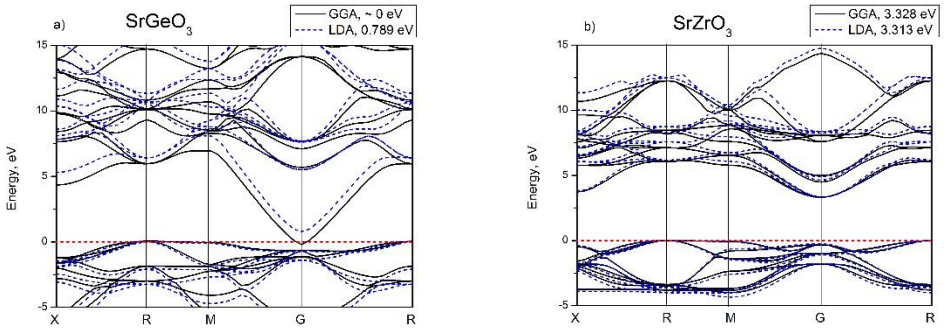

Fig. 4. Calculated electronic band structure for $SrGeO_3$ (a) and $SrZrO_3$ (b).

The calculated band gap values for $SrZrO_3$ (3.328 eV for the GGA calculations, and 3.313 eV for the LDA calculations) are consistent with others reported in the literature: 3.413 eV [42], 3.31 [43]. The calculated band values for $SrGeO_3$ (~0 eV for the GGA calculations, and 0.789 eV for the LDA calculations) are smaller than the reported value of 2.84 eV in Ref. [39], but it should be emphasized that the authors of Ref. [39] used the hybrid DFT method, which improves agreement with the experimental band gap values. The lowest states in the conduction band are highly dispersive, whereas the states from the valence band top are nearly flat, at least in the vicinity of the R and G points.

The band gaps are of indirect character for both studied materials. The origin and composition of the calculated electronic bands becomes clear after a careful examination of the density of states (DOS) diagrams from Fig. 5.

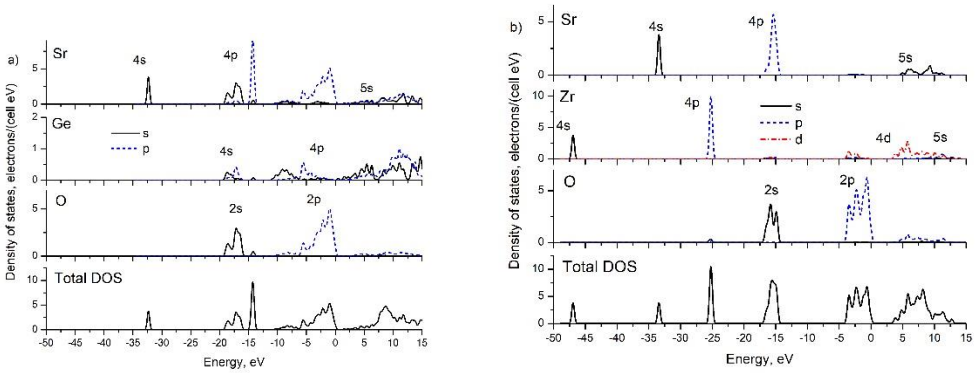

Fig. 5. Calculated density of states diagrams for $SrGeO_3$ (a) and $SrZrO_3$ (b).

The valence bands in both compounds are mainly composed of the oxygen 2p states. The conduction band in $SrGeO_3$ is made by the Sr 5s states with a minor

contribution from the Ge 4s, 4p states. The conduction band in $SrZrO_3$ consists of the Sr 5s states and Zr 4d, 5s states. The Sr 4s, 4p states produce sharply peaked maxima at about -33 eV and -15 eV, respectively. The O 2s states are located at about -17 eV in $SrGeO_3$ and at about -15 eV in $SrZrO_3$. The Zr 4s and 4p states are located deeply at -47 and -25 eV in $SrZrO_3$, whereas the Ge 4s, 4p states are at much higher energies in $SrGeO_3$.

The chemical bonding properties can be analyzed by considering the effective Mulliken charges and Mulliken bond orders. Because of formation of chemical bonds between ions in solids, the effective charges differ from those ones prescribed by their formal valences. Thus, the calculated charges of all ions in $SrGeO_3$ are (in units of the proton charge, GGA/LDA results are listed): Sr +1.01/+0.97; Ge +1.72/+1.70; O -0.91/-0.89. The same values for $SrZrO_3$ are: Sr +1.40/+1.36; Zr +1.07/+1.01; O -0.82/-0.79. The charges of the Sr ions are close to the formal value of +2, which indicates a mostly ionic Sr – O bonding, whereas the Ge – O and Zr – O bonds are more covalent in comparison with the Sr – O case. The larger value of the bond order corresponds to the covalent character of the considered bond, whereas its lower values indicate the ionic nature of the bond [46]. Thus, the Zr – O bond orders in $SrZrO_3$ are 0.86/0.84, whereas the Ge – O bond orders in $SrGeO_3$ are 0.86/0.88, indicating approximately comparable degree of covalency of those bonds. The values of the Sr – O bonds are 0.13/0.14 in $SrZrO_3$ and 0.18/0.18 in $SrGeO_3$, which is another indicator of highly ionic bonding in these cases.

3.3. Elastic properties

In addition to the extraction of the bulk moduli from the Murnaghan equation of state, direct calculations of the elastic constants were performed at the ambient and elevated pressures. The elastic properties of a solid are described by a 6×6 matrix of its elastic constants C_{ij}. In the case of a cubic crystalline solid, only three elastic constants are needed: C_{11}, C_{12}, C_{44}, with the following relations: $C_{11} = C_{22} = C_{33}$, $C_{12} = C_{23} = C_{31}$, $C_{44} = C_{55} = C_{66}$, and all remaining constants not listed here are equal to zero [47].

The calculated elastic constants values at the ambient pressure are collected in Table 2.

Table 2) Calculated and experimental elastic constants (in GPa) for $SrGeO_3$ and $SrZrO_3$ cubic perovskites.

	Calc. (this work, GGA/LDA)				*Calc. (other works)*			
	C_{11}	C_{12}	C_{44}	B	C_{11}	C_{12}	C_{44}	B
$SrGeO_3$	284/373	96/130	138/130	158/211	-	-	-	-
$SrZrO_3$	309/367	73/76	74/76	152/173	310[a], 309[b], 307[c], 339[d]	72[a], 71[b], 68[c], 71[d]	74[a], 74[b], 74[c], 77[d]	151[a], 155[b], 148[c], 160[d]

[a] Ref. [41] [b] Ref. [42] [c] Ref. [44] [d] Ref. [48]

No other data for $SrGeO_3$ were found in the literature, but high consistency between our calculated values and other results for $SrZrO_3$ allows to consider the $SrGeO_3$ values to be reliable.

It is worthwhile mentioning that the values of the bulk moduli B derived from the "volume – pressure" dependence in Fig. 3 are in good agreement with the data from Table 2.

Fig. 6 shows the behavior of all calculated lattice constants with increased pressure. The calculated values are shown by the symbols (solid ones for the GGA values, open ones for the LDA values). All data were linearly fitted; the fit lines are shown as solid for the GGA data and dashed for the LDA data. The linear fits equations are collected in Table 3.

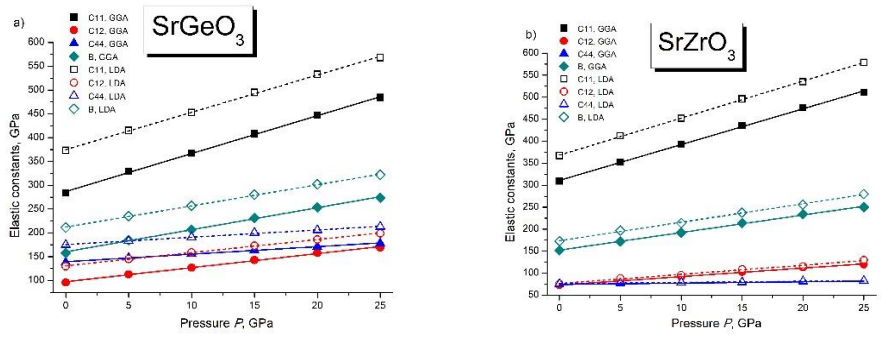

Fig. 6. Calculated elastic constants as the functions of external hydrostatic pressure for $SrGeO_3$ (a) and $SrZrO_3$ (b). See the text for more details.

Table 3) Dependences of elastic constants on pressure *P* (in GPa) for $SrGeO_3$ and $SrZrO_3$ cubic perovskites (equations of straight lines from Fig. 6).

	$SrGeO_3$		$SrZrO_3$	
	GGA	*LDA*	*GGA*	*LDA*
C_{11}	286.9 + 8.0 *P*	374.9 + 7.8 *P*	311.0 + 8.1 *P*	368.3 + 8.4 *P*
C_{12}	97.5 + 3.0 *P*	130.9 + 2.8 *P*	73.0 + 1.9 *P*	76.7 + 2.1 *P*
C_{44}	139.4 + 1.6 *P*	175.5 + 1.5 *P*	74.4 + 0.3 *P*	76.2 + 0.3 *P*
B	160.2 + 4.6 *P*	212.2 + 4.5 *P*	152.5 + 4.0 *P*	173.8 + 4.2 *P*

Equations given in Table 3 allow for a reliable estimation of the elastic constants at any value of the external hydrostatic pressure in the range from 0 to 25 GPa.

3.4. Thermodynamic properties

After the values of the elastic constants for a given solid are determined, it is possible to estimate the Debye temperature Θ_D, which is one of very important parameters of solids, proportional to the highest energy of the acoustic phonons. The following equations can be used [47,49,50]:

$$\Theta_D = \frac{h}{k}\left[\frac{3n}{4\pi}\left(\frac{N_A\rho}{M}\right)\right]^{1/3} v_m, \tag{2}$$

where *h* and *k* are the Planck's and Boltzmann's constants, N_A is the Avogadro's number, ρ stands for the crystal's density, *M* equals to the molecular weight, and *n* is the number of atoms per one formula unit (five in this case). The last entry, v_m, is the mean sound velocity, which can be calculated if the longitudinal v_l and transverse v_t sound velocities are known:

$$v_m = \left[\frac{1}{3}\left(\frac{2}{v_t^3} + \frac{1}{v_l^3}\right)\right]^{-1/3}, \tag{3}$$

$$v_l = \sqrt{\frac{3B+4G}{3\rho}},\ v_t = \sqrt{\frac{G}{\rho}}, \tag{4}$$

B is the bulk modulus, $G = \frac{G_V+G_R}{2}$ is the isotropic shear modulus, which is an average of the Voight's shear modulus G_V and the Reuss's shear modulus G_R. These parameters are expressed in terms of the elastic constants C_{ij} as:

$$G_V = \frac{C_{11}-C_{12}+3C_{44}}{5}, \frac{5}{G_R} = \frac{4}{C_{11}-C_{12}} + \frac{3}{C_{44}}, \tag{5}$$

Application of Eqs. (2) – (5) to the calculated data on the elastic constants resulted in the values of the densities, sound velocities and Debye temperatures collected in Tables 4-5.

Table 4) Calculated density ρ (kg/m^3), sound velocities v_t, v_l, v_m (m/s) Debye temperatures Θ_D (in K) for different hydrostatic pressures P (in GPa) in $SrGeO_3$ cubic perovskite.

P	GGA					LDA				
	ρ	v_t	v_l	v_m	Θ_D	ρ	v_t	v_l	v_m	Θ_D
0	6028	4430	7237	4891	646	6657	4766	7873	5268	719
5	6206	4585	7605	5069	676	6807	4878	8140	5397	742
10	6365	4697	7870	5199	699	6946	4976	8367	5509	763
15	6511	4809	8143	5328	722	7077	5090	8609	5639	786
20	6647	4904	8383	5438	742	7199	5169	8808	5730	803
25	6774	5002	8591	5549	762	7315	5243	8982	5815	819

Table 5) Calculated density ρ (kg/m^3), sound velocities v_t, v_l, v_m (m/s) Debye temperatures Θ_D (in K) for different hydrostatic pressures P (in GPa) in $SrZrO_3$ cubic perovskite.

P	GGA					LDA				
	ρ	v_t	v_l	v_m	Θ_D	ρ	v_t	v_l	v_m	Θ_D
0	5188	4148	7228	4608	563	5482	4247	7457	4720	587
5	5351	4232	7485	4707	581	5631	4315	7734	4805	603
10	5499	4303	7720	4791	596	5769	4369	7908	4868	616
15	5636	4355	7954	4856	609	5898	4415	8145	4927	628
20	5763	4405	8153	4916	622	6018	4478	8323	5000	641
25	5883	4461	8308	4982	634	6132	4520	8538	5052	652

As seen from Tables 4-5, all calculated parameters increase with increased pressures. The Debye temperature increases linearly with pressure, as is evidenced by Fig. 7.

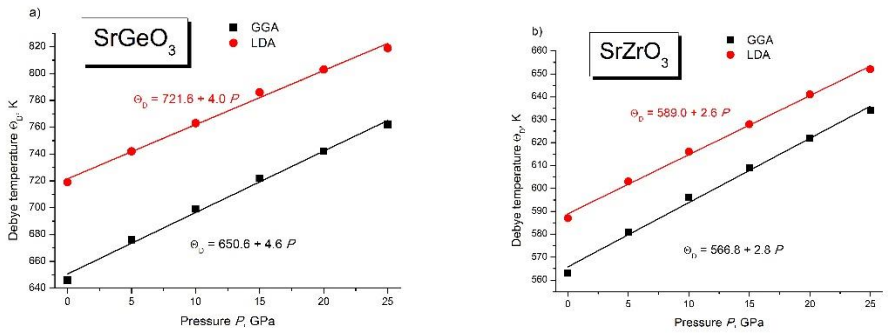

Fig. 7. Calculated Debye temperatures as the functions of external hydrostatic pressure for $SrGeO_3$ (a) and $SrZrO_3$ (b). The calculated values are shown by symbols, the linear fits are shown by straight lines. The fits equations are given in the graphs.

4. Conclusions

Detailed first-principles analysis of the pressure effects on the structural, electronic, elastic and thermodynamic properties of two cubic perovskites – $SrGeO_3$ and $SrZrO_3$ – was performed in the present paper. All calculated values – lattice constants, relative change of a unit cell volume, elastic constants, and Debye temperature – were fitted to the linear functions of pressure. The obtained dependencies allow to estimate all these quantities for any value of pressure in the studied range from 0 to 25 GPa.

Acknowledgment

M.G.B. thanks the supports from the Chongqing Recruitment Program for 100 Overseas Innovative Talents (Grant No. 2015013), the Program for the Foreign Experts (Grant No. W2017011) and Wenfeng High-end Talents Project (Grant No. W2016-01) offered by Chongqing University of Posts and Telecommunications (CQUPT), Estonian Research Council grant PUT PRG111, European Regional Development Fund (TK141) and NCN project 2018/31/B/ST4/00924. Dr. G.A. Kumar, University of Texas, San Antonio, is thanked for allowing to use Materials Studio.

References

[1] A. S. Bhalla, R.Y. Guo, R. Roy, Mater. Res. Innov. **4**, 3 (2000).
[2] W. Travis, E.N. K. Glover, H. Bronstein, *et al.*, Chem. Sci. **7**, 4548 (2016).
[3] B. Sarapov, D. B. Mitzi, Chem. Rev. **116**, 4558 (2016).
[4] J.B. Philipp, P. Majewski, L. Alff, *et al*., Phys. Rev. B **68**, 144431 (2003).
[5] J. Burschka, N. Pellet, S.-J. Moon, *et al*., Nature **499**, 316 (2013).
[6] S. Jin, T. H. Tiefel, M. McCormack, *et al*., Science **264**, 413 (1994).
[7] N. Q. Minh, J. Am. Ceram. Soc. **76**, 563 (1993).
[8] X.-M. Li, Y. Wu, S.-L. Zhang, *et al*., Adv. Funct. Mater. **26**, 2435 (2016).
[9] A. Grimaud, K. J. May, C. E. Carlton, *et al*., Nature Commun. **4**, 2439 (2013).
[10] M. Nikl, V. V. Laguta, A. Vedda, Phys. Stat. Solidi B **245**, 1701 (2008).
[11] Q.-S. Chen, J. Wu, X.-G. Ou, *et al*., Nature **561**, 88 (2018).
[12] E. Heifets, R. I. Eglitis, E. A. Kotomin, Phys. Rev. B **64**, 235417 (2001).
[13] S. Piskunov, E. A. Kotomin, E. Heifets, *et al*., Surf. Sci. **575**, 75 (2005).
[14] R. I. Eglitis, A. I. Popov, J. Saud. Chem. Soc. **22**, 459 (2018).
[15] R. I. Eglitis, Int. J. Mod. Phys. B **28**, 1430009 (2014).
[16] S. Saha, T. P. Sinha, A. Mookerjee, Phys. Rev. B **62**, 8828 (2000).

[17] K. van Benthem, C. Elsasser, R. H. French, J. Appl. Phys. **90**, 6156 (2001).
[18] S. Piskunov, E. Heifets, R. I. Eglitis, *et al*., Comput. Mater. Sci. **29**, 165 (2004).
[19] K. Khan, J. Sahariya, A. Soni, Mater. Chem. Phys. **262**, 124284 (2021).
[20] A. R. Oganov, C. W. Glass, J. Chem. Phys. **124**, 244704 (2006).
[21] S. Ono, A. R. Oganov, Earth Planet. Sci. Lett. **236**, 914 (2005).
[22] M. G. Brik, J. Phys.: Condens. Matter **21**, 485502 (2009).
[23] M. G. Brik, C.-G. Ma, Comput. Mater. Sci. **51**, 380 (2012).
[24] C.-G. Ma, D.X. Liu, B. Feng, *et al*., J. Lumin. **169**, 415 (2016).
[25] L. Li, Y.-J. Wang, D.-X. Liu, *et al*., Mater. Chem. Phys. **188**, 39 (2017).
[26] Y. Wang, W.-B. Chen, F.-Y. Liu, *et al*., Res. Phys. **13**, 102180 (2019).
[27] Y. Li, B. Xiao, Y. Tang, *et al*., J. Phys. Chem. C **124**, 28458 (2020).
[28] B. Wu, M.-L. Yang, Y.-C. Yan, *et al*., J. Am. Cer. Soc. **104**, 1489 (2021).
[29] A. Nakatsuka, A. Yoshiasa, K. Fujiwara, *et al*., J. Miner. Petr. Sci. **113**, 280 (2018).
[30] H. D. Megaw, Proc. Phys. Soc. Lond. **58**, 133 (1946).
[31] S.J. Clark, M.D. Segall, C.J. Pickard, *et al*., Z. Krist. **220**, 567 (2005).
[32] J.P. Perdew, K. Burke, M. Ernzerhof, Phys. Rev. Lett. **77**, 3865 (1996).
[33] D.M. Ceperley, B.J. Alder, Phys. Rev. Lett. **45**, 566 (1980).
[34] J.P. Perdew, A. Zunger, Phys. Rev. B **23**, 5048 (1981).
[35] K. Momma, F. Izumi, J. Appl. Crystallogr. **44** 1272 (2011).
[36] R. D. Shannon, Acta Crystall. A **32**, 751 (1976).
[37] C. H. Kronbo, F. Menescardi, D. Ceresoli *et al*., J. Alloys Compds. **855**, 157419 (2021).
[38] Y. Wang, W. Tang, J. Cheng, *et al*., Phys. Chem. Chem. Phys. **18**, 31924 (2016).
[39] A. J. E. Rowberg, K. Krishnaswamy, C. G. Van de Walle, Semicond. Sci. Technol. **35**, 085030 (2020).
[40] A. Grzechnik, A. V. G. Chizmeshaya, G. H. Wolf *et al*., J. Phys.: Condens. Matter **10**, 221 (1998).
[41] I. R. Shein, V. L. Kozhevnikov, A. L. Ivanovskii, Solid State Sci. **10**, 219 (2008).
[42] M. A. Ghebouli, T. Chihi, F. Dahmane, *et al*., Chin. J. Phys. **56**, 1514 (2018).
[43]L. Weston, A. Janotti, X. Y. Cui, *et al*., Phys. Rev. B **92**, 085201 (2015).
[44] L.-W. Shi, Y.-F. Duan, X.-Q. Yang, *et al*., Chin. Phys. Lett. **27**, 096201 (2010).
[45] F.D. Murnaghan, Proc. Natl. Ac. Sci. **30**, 244 (1944).
[46] M.D. Segall, R. Shah, C.J. Pickard, *et al*., Phys. Rev. B **54**, 16317 (1996).
[47] J.-P. Poirier, Introduction to the Physics of the Earth's Interior, Cambridge University Press, 2000.
[48] R. Terki, H. Feraoun, G. Bertrand, *et al*., Phys. Stat. Sol. (b) **242**, 1054 (2005).
[49] O.L. Anderson, J. Phys. Chem. Solids **24**, (1963) 909.
[50] E. Schreiber, O.L. Anderson, N. Soga, Elastic Constants and Their Measurements, McGraw-Hill, New York, 1973.